^{40}Ar–^{39}Ar isotope constraints on the age of deformation in Charnwood Forest, UK

J. N. CARNEY[*][†], P. ALEXANDRE[‡], M. S. PRINGLE[§], T. C. PHARAOH[*],
R. J. MERRIMAN[*] & S. J. KEMP[*]

[*]British Geological Survey, Kingsley Dunham Centre, Keyworth, Nottingham NG12 5GG, UK
[‡]Scottish Universities Environmental Research Centre, Rankine Avenue, East Kilbride, Scotland G75 OQF, UK
[§]Massachusetts Institute of Technology, Dept. Earth, Atmospheric and Planetary Sciences,
Cambridge, MA 02139-4307, USA

Abstract – ^{40}Ar–^{39}Ar dating by a combination of spot analysis and step-heating has been carried out on mica fabrics from slaty cleavage and a shear zone in the Neoproterozoic to Cambrian rocks of Charnwood Forest, Leicestershire. The results indicate that crust adjacent to the eastern margin of the Midlands Microcraton was affected by localized epizonal metamorphism and penetrative deformation between 425 and 416 Ma (Silurian to earliest Devonian), somewhat earlier than the Acadian Phase of the Caledonian orogeny recorded elsewhere in southern Britain. The Charnwood cleavage geometry suggests that the deformation arose within a dextral transpressional regime along the eastern margin of the Midlands Microcraton. This tectonism may have overlapped with pre-Acadian sinistral transtensional movements documented for the Welsh Basin and Lake District areas, to the west and north of the Midlands Microcraton.

Keywords: argon, Acadian, Caledonian, deformation.

1. Introduction

Charnwood Forest forms the westernmost edge of a basement domain known in England as the 'Eastern Caledonides' (Pharaoh *et al*. 1987). This domain is contiguous with the Caledonian terranes concealed beneath eastern England and the North Sea, and exposed in NW Europe within the Brabant and Ardennes massifs of Belgium (Pharaoh, 1999), attributed to the Anglo-Brabant Deformation Belt (Winchester, Pharaoh & Verniers, 2002). The study area (Fig. 1a) borders a major tectonic interface with the Midlands Microcraton, a triangular-shaped crustal block (Turner, 1949) bounded by major faults and mainly composed of latest Neoproterozoic igneous and volcaniclastic rocks overlain by strata of Early Palaeozoic through to Mesozoic age. In plate tectonic terms, the microcraton forms a relatively rigid structural entity that separates the Eastern Caledonides from the Neoproterozoic and Early Palaeozoic basement terranes of England, Wales and SW Ireland, which prior to the opening of the Atlantic Ocean were contiguous with the 'Avalonian' provinces of eastern Canada and the USA.

The microcraton interior has escaped widespread penetrative deformation internally, but against its eastern margin, in Charnwood Forest, there is developed a pervasive cleavage fabric that up until now has not been the subject of a specific geochronological study. K–Ar whole-rock ages determined previously for various Charnian units (Meneisy & Miller, 1963) have yielded a broad spread of values, ranging from Neo-proterozoic (684 ± 29 Ma to 574 ± 25 Ma) through to Ordovician (472 ± 21 Ma to 438 ± 20 Ma), Silurian–Devonian (416 ± 19 Ma to 378 ± 17 Ma), and Permo-Carboniferous (318 ± 29 Ma to 260 ± 15 Ma). The fact that the Charnwood cleavage is imprinted on rocks that include the Swithland Formation, which is now thought to be Early Cambrian in age, indicates that it must be part of a Phanerozoic tectonic event.

In terms of a Phanerozoic deformational age, a likely candidate is the Caledonian orogeny, which in Britain to the south of the Iapetus suture is subdivided by McKerrow *et al*. (2000) into a number of discrete tectonic phases. The folding and penetrative cleavage that occurred during their 'Acadian Phase' are particularly well developed in the paratectonic Caledonides belts of the Welsh Basin, northern England and the Lake District, to the west and north of the Midlands Microcraton (Fig. 1a). In the wider plate tectonic context, the event has been related to the collision of some part of the Armorican Terrane Assemblage (e.g. see Winchester, Pharaoh & Verniers, 2002) with terranes comprising Laurussia that had previously been docked along the Iapetus closure line (Soper, Webb & Woodcock, 1987; Dewey & Strachan, 2003). In southern Britain, McKerrow, Mac Niocaill & Dewey (2000) refer the age of the Acadian Phase to mainly Devonian (Emsian) time. The Acadian Phase was, however, both preceded and accompanied by large-scale translational deformation (Soper & Woodcock, 2003), and evidence is presented here which suggests that similar types of displacement may have been focused along the eastern edge of the Midlands Microcraton.

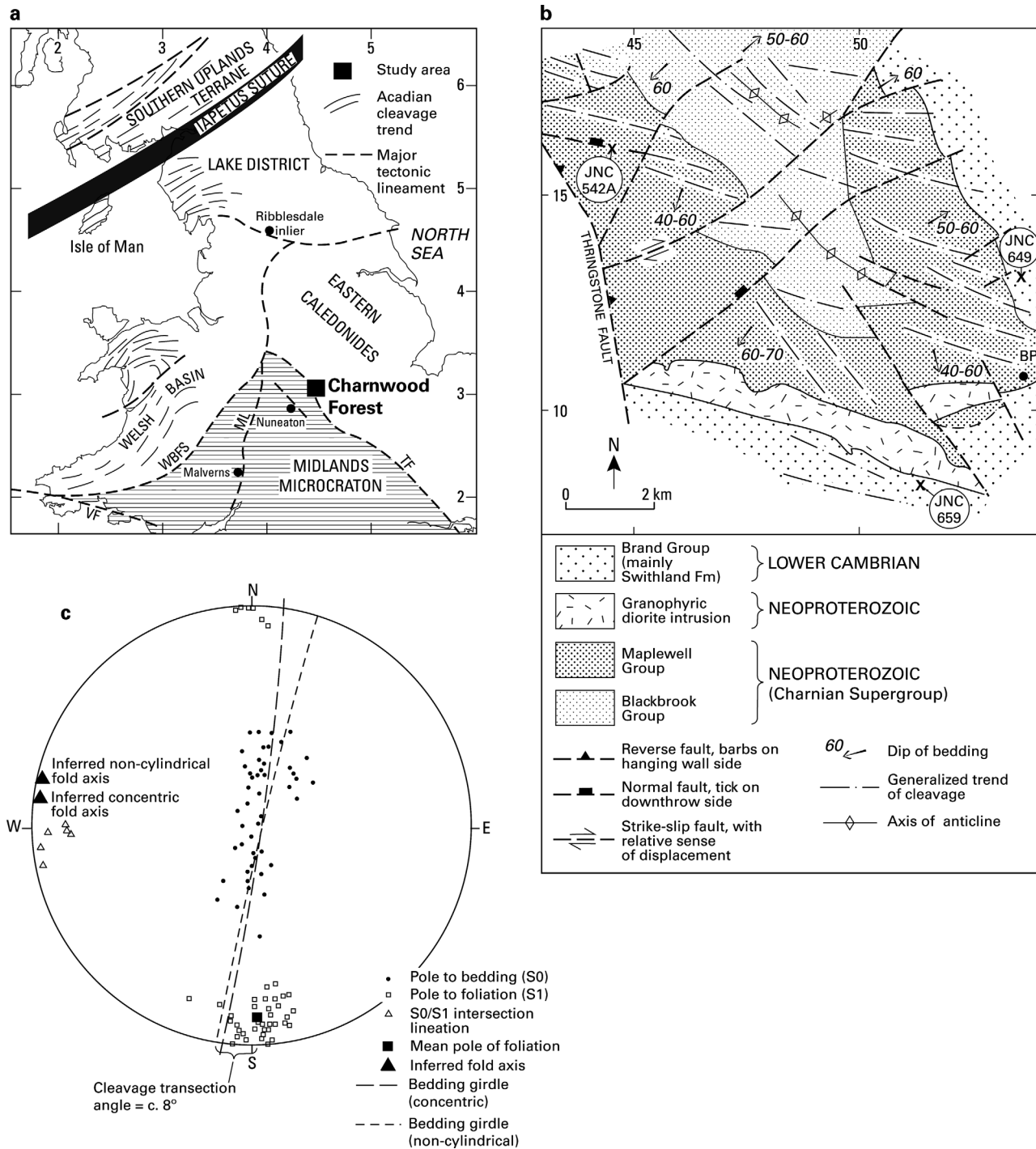†Author for correspondence: j.carney@bgs.ac.uk

Figure 1. Geological setting. (a) Regional tectonic setting of the Charnwood Forest study area, in part based on Soper, Webb & Woodcock (1987), Pharaoh & Carney (2000) and British Geological Survey (1996). ML – Malvern Lineament; TF – Thringstone Fault; VF – Variscan Front; WBFS – Welsh Borderland Fault System. (b) Charnwood Forest study area, with locations of the *in situ* samples (circled numbers) (modified from Carney, 1999). BP – Bradgate Park (grid is the British National Grid based on the Ordnance Survey map with the permission of The Controller of Her Majesty's Stationery Office Crown Copyright; licence number GD272191/2003). (c) Stereographic plot of structural data for folded Charnian bedding in the Maplewell Group (Bradgate Formation) east of Coppice Plantation at Bradgate Park (SK540 110), indicated as BP in (c). The inferred plunge of the measured fold axis is gently westward, comparable to observed bedding/foliation intersection lineations. The calculated cleavage transection angle is 8° anticlockwise.

2. Geological setting of Charnwood Forest samples

The rocks that have been sampled (Fig. 1b) are located within the Charnwood Forest inlier of basement rocks lying immediately to the east of the Midlands Microcraton, the tectonic boundary of which is defined by the Thringstone Fault (Smith, 1987; Lee, Pharaoh & Soper, 1990). The Charnwood cleavage is slightly sinusoidal, but with a predominant ESE strike (100° to 120°) that is for the most part oblique with respect to

Table 1. Summary petrographical features of the samples

Sample no.	NGR and locality	Lithostratigraphy	Lithology, microfabric, grade	Mica type	Mica max. length (mm)
JNC 649	SK 5376 1314 The Brand	Swithland Fm.: *in situ*	Volcaniclastic silty slate, *in situ*; approximately bedding-parallel microfabric. Epizone (KI = 0.18).	a:b:c ≈ 92:5:3	a: 0.15 b: 0.3
JNC 659	SK 5106 0828 Home Farm	Swithland Fm:, *in situ*	Sandy/silty slate, *in situ*; spaced disjunctive slaty cleavage microfabric. Epizone (KI = 0.23).	a:b:c ≈ 70:10:20	a: 0.08 b: 0.20 c: 0.04
JNC 662	SK 5132 0590 Ratby Church	Swithland Fm.: headstone	Silty slate (headstone) with numerous chlorite/mica stacks. Intense slaty cleavage with continuous microfabric.	a:b:c ≈ 90:5:5	a: 0.08 b: 0.08 c: 0.06
JNC 663	SK 5132 0590 Ratby Church	Swithland Fm.: headstone	Silty slate (headstone) with numerous chlorite/mica stacks. Intense slaty cleavage with continuous microfabric.	a:b:c ≈ 90:5:5	a: 0.08 b: 0.08
JNC 542A	SK 4485 1614 Whitwick Quarry	Charnian S'group.: ductile shear	Phyllonite. Continuous microfabric of oriented white mica; quartz+ feldspar mosaics also partly oriented. Some late veins have poorly oriented white mica and chlorite. Epizone (KI = 0.24).	a:c ≈ 80:20	a: 0.010 c: 0.006

Mica types: a – fabric-forming; b – detrital; c – replacive.

the SE axial trend of the main Charnwood anticline. It is imprinted on volcanic and volcaniclastic rocks of the Charnian Supergroup (Moseley & Ford, 1985), of latest Neoproterozoic age, as well as on the sequence of silty mudrocks that comprises the overlying Swithland Formation (Brand Group). It had long been assumed that all of the Charnwood Forest basement rocks were Neoproterozoic in age; however, it is now thought that the Swithland Formation is significantly younger than this. In many local churchyards, headstones carved from the Swithland Formation have yielded trace fossils (*Teichichnus*) indicative of a Phanerozoic, possibly Early Cambrian age (Bland & Goldring, 1995; McIlroy, Brasier & Moseley, 1998).

All of the samples are characterized by an intense, millimetre- or micron-scale cleavage, as described in Table 1. It is therefore anticipated that the isotope determinations will include the age of the fabric-forming event in both the Swithland Formation and the underlying Charnian Supergroup. The *in situ* samples (Fig. 1b) are from three different structural settings. Samples JNC 649 and JNC 659 are silty mudstones with abundant detrital quartz and albitized feldspar grains. They were collected from disused quarries in the Swithland Formation at geographically separated localities, respectively on the eastern and western limbs of the Charnwood anticline, in order to minimize bias caused by local and possibly aberrant lithological and/or tectonic conditions. A further *in situ* sample (JNC 542A, Table 1) is a silvery, strongly foliated and weakly lineated, highly micaceous rock (phyllonite) from a composite brittle/ductile fault zone cutting a Charnian porphyritic dacite in Whitwick Quarry. The ESE orientation of this fault zone is parallel to the regional cleavage (Carney, 2005), suggesting that faulting and cleavage formation were contemporary, and that strain during the cleavage-forming event may have been heterogeneously distributed. The value of this sample is that, because its protolith was a primary igneous rock, it will be devoid of detrital mica contaminant grains.

Two further Swithland Formation samples (JNC 662, 663; Table 1) are not *in situ*; they were collected as small, fresh cleavage flakes from the crumbled corners of headstones in Ratby churchyard, to the south of the Charnwood study area shown in Figure 1b. They were included in this study because the headstones have been quarried from the best quality local slate resource, which we have found to be particularly pure in terms of their high original mud content. In many quarries, such material occurred in narrow, subvertical 'seams', less than 5 m wide, which are now inaccessible due to flooding of the quarries. The headstones are also of major significance to the stratigraphy of Charnwood Forest, as noted previously.

3. Metamorphic conditions

X-ray diffraction (XRD) techniques were used to determine the Kübler indices of white mica (illite) 'crystallinity'. The Kübler index (KI in $\Delta°2\theta$) measures small reductions in the half-height width of the dioctahedral mica ~ 10 ÅXRD peak resulting from crystallite thickening during reaction progress in the smectite–illite–muscovite series (Merriman & Peacor, 1999). White mica crystallite thickness generally increases with grade, a process accelerated during slaty cleavage development, so that the mean thickness of epizonal mica would be expected to exceed 520 Å, whereas anchizonal white micas have mean thicknesses in the range 230–520 Å(Merriman & Peacor, 1999). These crystallographic changes can be used to measure the progress of advancing metamorphic grade (Merriman, Roberts & Peacor, 1990; Merriman *et al.* 1995*a*; Warr & Rice, 1994). In pelitic rocks, KI values are used to define the limits of a series of metapelitic zones of very low- and low-grade metamorphism: diagenetic zone (KI > 0.42), anchizone (KI 0.42–0.25) and epizone (KI < 0.25) (Kisch, 1990).

For the northern part of the Charnwood Forest area shown in Figure 1b, a metamorphic zonation was previously determined by Merriman & Kemp (1997),

based on the distribution of mean values and the range of KI data for 71 samples. The near-ubiquitous development of epizonal KI values, which are seen in the data for the Swithland Formation samples analysed for this study (Table 1), reflects the well-developed tectonic fabric of mica-rich rocks in the Charnwood basement, and suggests that white mica recrystallization is strain-enhanced (note that due to the small size of the samples, KI determinations could not be carried out for the headstone rocks JNC 662 and 663). The highest grades indicate temperatures of 300–350 °C, corresponding to burial depths of up to 10 km. The Charnwood shear zone rock (JNC 542A; Table 1) shows slightly lower grades than the *in situ* slates and this may reflect retrogression or comminution of white mica crystallites caused by high strain rates and sluggish recovery following ductile deformation (Kemp & Merriman, 1995).

4. Petrography and mica fabrics

Three petrographic types of white mica have been distinguished and their estimated proportions, along with other summary data for the samples, are shown in Table 1. Type (a) fabric-forming micas (Fig. 2a–c) are found as intergrowths with chlorite in the orientated microstructural P-domains that define the slaty cleavage (Knipe, 1981). Estimates of their maximum length (Table 1) are based on measurements made on apparently optically continuous grains. The uncertainties of resolving crystallographic continuity in mica–chlorite intergrowths on this scale by optical methods, however, underlines the approximate nature of the measurements. Type (b) detrital micas (Fig. 2c) include the white mica within chlorite–mica stacks. Although these stacks are of detrital origin, both their white mica and chlorite minerals probably developed during late diagenesis and burial (e.g. Li *et al.* 1994). Type (c) replacive white mica was generated by secondary processes pre-dating the fabric-forming event, and does not show a preferred orientation. It includes mica replacing crystal, vitric and lithic volcanic grains, and grain coatings representing recrystallized matrix clay mica.

In terms of their relative ages, type (a) white micas that define the slaty cleavage microfabric are the most recently formed and would be expected to give ages that approximate to the fabric-forming event. Type (b) detrital micas are assumed to have been derived from contemporary basement outcrop at the time of sedimentary accumulation and would be expected to give the oldest ages. As the degree of tectonic fabric formation increases with grade, however, more detrital micas are likely to have recrystallized into the cleavage domains (e.g. Ho, Peacor & van der Pluijm, 1999; Van de Pluijm *et al.* 1998) and therefore in epizonal grade samples such as those from Charnwood Forest, a high proportion of the detrital mica population is likely to have isotopically equilibrated under the metamorphic conditions that generated the tectonic fabric-forming
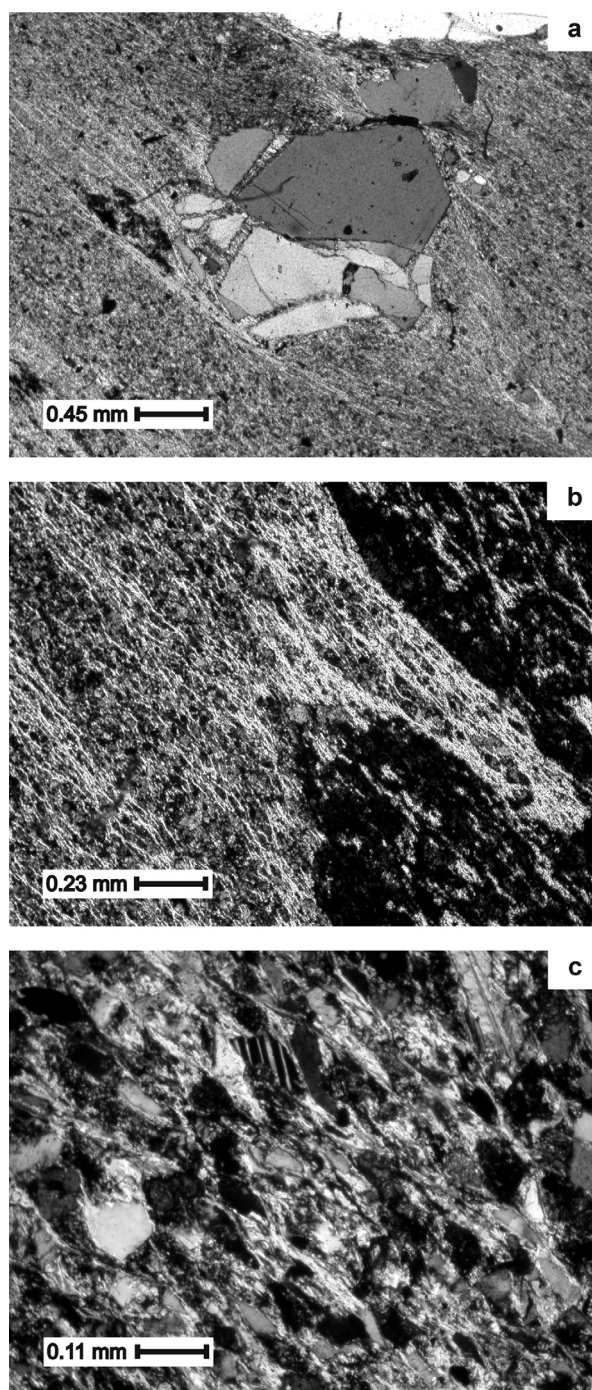
Figure 2. Photomicrographs of dated samples of Charnian slates and phyllonite. (a) Sample JNC 542A: continuous, non-domainal slaty cleavage in phyllonite. Note penetration of fabric into fractures in quartz phenocryst; crossed polarizers. (b) Sample JNC 542A: continuous, anastomosing slaty cleavage in phyllonite matrix; crossed polarizers. (c) Sample JNC 649: domainal cleavage in siltstone sample JNC 649; many of the larger, detrital clasts show pressure-solution textures; crossed polarizers.

micas (e.g. Dong *et al.* 1997). It is noted that the muscovite closure temperature for argon is generally about 500 °C (Villa, 1998); however, given that the grains measured for this study are relatively small (typically less than 100 μm; Fig. 2 and Table 1), the closure temperature for the studied micas would be

somewhat lower, for instance, 400 to 450 °C, or even lower (300 to 350 °C) if the calculations of Parry *et al.* (2001) are to be followed. These estimates for the closure temperature of the dated muscovite are therefore similar or to higher than the metamorphic temperatures. The detrital population may not be completely reset, however, as indicated by previously determined age ranges for Welsh Basin epizonal slates reviewed by Sherlock *et al.* (2003). As already noted, detrital mica will be absent from the ductile shear zone sample (JNC 542A), which cuts dacitic rocks of primary igneous origin. Type (c) replacive white mica, because of its very fine grain size, has almost certainly equilibrated to the metamorphic conditions prevailing during fabric formation. In terms of ^{40}Ar–^{39}Ar isotope systematics, this type of mica would have formed closed systems at the same time as the fabric-forming mica.

All samples possess an intense slaty cleavage microfabric comprising orientated intergrowths of white mica and chlorite. In the phyllonite (ductile shear) sample JNC 542A, a continuous non-domainal fabric is developed, which may penetrate fractures in some granulated, relict quartz phenocrysts (Fig. 2a). Although the cleavage is domainal in character in the siltstone sample JNC 649, pressure-solution has elongated most detrital grains into the penetrative fabric (Fig. 2c). The penetrative development of the microfabric is reflected in the epizonal grade of the Charnwood samples, and in the relatively low proportions of type (b) and type (c) micas (less than 10 % and 20 %, respectively; Table 1). Nevertheless, a few detrital micas have survived in the slates (Fig. 2c).

5. Analytical methods

Thin slices of about $5 \times 10 \times 0.2$ mm were cut from the various lithologies, polished on one side, and cleaned in acetone in an ultrasonic bath. They were then wrapped individually in aluminium foil, and irradiated for 120 hours in the Oregon State University TRIGA reactor. The neutron flux was measured with mineral standards wrapped in aluminium foil and surrounding and intercalated between the sample packets. Its variability is known down to approximately ± 0.3 % relative (1σ) at any point on the rock slices, and is mainly due to the horizontal flux gradient across the sample rock slice. The uncertainty of the measured neutron flux is propagated into the final weighted average ages (for spot fusion) and plateau ages (for incremental heating) and typically contributes to less than 30 % of the age uncertainty. Absolute ages are reported relative to the biotite standard GA1550 (98.79 ± 0.96 Ma; McDougall & Roksandic, 1974; Renne *et al.* 1998).

Argon was extracted from the samples by both laser spot fusion and incremental heating techniques at the Scottish Universities Environmental Research Centre. For the spot fusion analyses, argon was extracted from up to 12 spots per sample, chosen in areas of the rock slices with the finest grain sizes (to avoid

detrital micas) and highest mica contents (to avoid other mineral phases). Heating was accomplished with a 65W CW Nd-YAG laser beam focused through a modified petrographic microscope and shuttered externally in 5 to 10 bursts of 0.1 second to minimize heating of the surrounding sample. The resulting fusion pits were generally less than 200 μm in diameter and went through the thickness of the rock slice. For the incremental heating analyses, carefully selected chips of the rock slices measuring about 0.5 mm^2 were heated for 120 seconds for each step with a defocused 25W CO_2 laser beam of about 1.5 mm in diameter. Power levels for each step ranged from a nominal 1.3 to 8.0 % of full power, corresponding to 0.3 to 2 W.

The released gas was purified after heating for 7 to 8 minutes with two SAES Zr–Al GP50 getters, one operated at about 400 °C and the other at room temperature, as well as with an off-line stainless steel finger cooled with an acetone and dry ice slush. For the spot fusion analyses, the cleaned gas was measured with a MAP-215 mass spectrometer using a fixed slit giving a resolution of about 300, and an electron multiplier operated at a gain of about 4000. For the incremental heating analyses, the cleaned gas was measured with a MAP-215/50 mass spectrometer using an adjustable slit set to a resolution of about 600 and a Johnson MM-1 electron multiplier operated at a gain of about 15 000. The raw argon data were corrected for total system blank, reactor-induced mass interferences, mass fractionation and ^{39}Ar and ^{37}Ar decay. Individual ^{40}Ar–^{39}Ar age and error calculations follow Dalrymple *et al.* (1981), and all analytical uncertainty margins are reported at the 1σ level.

6. ^{40}Ar–^{39}Ar analytical data

The full analytical data are presented in Table 2 and are separated into two groups as a function of the extraction method: 52 spot fusion analyses (summarized in Fig. 3) and six step heating analyses (Fig. 4). The ages (at the 1σ confidence level) are hereafter presented, treated, and compared on the basis of a separation into: Swithland Formation *in situ* rocks (JNC 649 and JNC 659), Swithland Formation headstones (JNC 662 and JNC 663), and the Charnian ductile shear zone phyllonite (JNC 542A). The statistical treatment used for the spot fusion results was the cumulated probability analysis (e.g. Alexandre *et al.* 2004); it was used in order to obtain age group distributions and therefore age information. One of the advantages of this method is that there is no choice of bin width, as in classical histograms, but of how often the probability is calculated, the only effect of which is the smoothness of the final curve. In our case, probability was calculated every 1 Ma, ensuring that the overall shape of the curve is not affected at all by any calculation bias, as the error margin of each age used for the calculation is significantly higher than 1 Ma (Table 2). The individual age probabilities (assuming Gaussian distribution) were integrated over

Table 2. Results of the ^{40}Ar/^{39}Ar analyses of the samples from the studied Charnwood samples

Sample Rock or mineral	Step	^{36}Ar/^{40}Ar	±1σ	^{39}Ar/^{40}Ar	±1σ	Ca/K	^{40}Ar air (%)	^{39}Ar (%)		^{40}Ar*/^{39}Ar$_K$	±1σ	Age (Ma)	±1σ
Total fusion spot experiments													
JNC 649	TF1	0.00009	0.00001	0.07937	0.00239	0.287	2.5	1.5	1.5	12.283	0.252	433.8	8.9
Siltstone	TF2	0.00008	0.00000	0.07586	0.01836	0.173	2.2	2.7	4.2	12.888	0.145	452.7	5.1
	TF3	0.00007	0.00004	0.08113	0.00048	0.184	2.1	2.5	6.7	12.073	0.155	427.2	5.5
Average age:	TF4	0.00011	0.00004	0.07872	0.00072	0.211	3.0	2.9	9.6	12.318	0.161	434.9	5.7
424.4 ± 1.5 Ma	TF5	0.00012	0.00010	0.07927	0.00034	0.199	3.4	3.0	12.6	12.185	0.136	430.7	4.8
	TF6	0.00013	0.00008	0.07911	0.00045	0.174	3.7	3.1	15.7	12.169	0.133	430.2	4.7
	TF7	0.00003	0.00002	0.08097	0.00033	0.135	0.8	4.7	20.4	12.251	0.099	432.8	3.5
	TF8	0.00003	0.00004	0.08371	0.00024	0.250	0.8	9.9	30.3	11.858	0.056	420.4	2.0
	TF9	0.00006	0.00005	0.08114	0.00037	0.145	1.8	4.9	35.2	12.099	0.088	428.0	3.1
	TF10	0.00006	0.00007	0.08264	0.00027	0.208	1.7	64.7	100.0	11.893	0.042	421.5	1.5
JNC 659	TF1	0.00004	0.00005	0.08148	0.00022	0.068	1.2	1.0	1.0	12.124	0.170	428.8	6.0
Siltstone	TF2	0.00107	0.00118	0.05504	0.00018	0.051	31.7	1.3	2.3	12.408	0.181	437.7	6.4
	TF3	0.00150	0.00087	0.04735	0.00029	0.053	44.3	0.5	2.8	11.769	0.581	417.6	20.6
Average age:	TF4	0.00002	0.00003	0.07974	0.00023	0.018	0.7	0.9	3.7	12.456	0.170	439.2	6.0
434.6 ± 1.5 Ma	TF5	0.00012	0.00009	0.08126	0.00040	0.082	3.5	0.7	4.4	11.874	0.257	420.9	9.1
	TF6	0.00009	0.00011	0.07697	0.00023	0.045	2.8	1.3	5.7	12.632	0.148	444.7	5.2
	TF7	0.00007	0.00005	0.07939	0.00038	0.060	2.0	62.4	68.1	12.347	0.040	435.8	1.4
	TF8	0.00003	0.00003	0.07943	0.00028	0.056	0.8	25.0	93.1	12.481	0.043	440.0	1.5
	TF9	0.00006	0.00001	0.08651	0.00256	0.049	1.8	6.8	100.0	11.345	0.053	404.1	1.9
JNC 662	TF1	0.00007	0.00004	0.08442	0.00047	0.028	2.0	1.5	1.5	11.609	0.166	412.5	5.9
Slate	TF2	0.00009	0.00002	0.08243	0.00150	0.063	2.6	1.6	3.1	11.811	0.135	418.9	4.8
	TF3	0.00002	0.00001	0.08519	0.00037	0.063	0.4	1.6	4.7	11.687	0.113	415.0	4.0
Average age:	TF4	0.00004	0.00002	0.08386	0.00064	0.049	1.2	1.8	6.5	11.779	0.118	417.9	4.2
412.7 ± 1.7 Ma	TF5	0.00012	0.00007	0.08384	0.00053	0.056	3.4	1.5	8.0	11.521	0.169	409.7	6.0
	TF6	0.00009	0.00005	0.08535	0.00056	0.086	2.7	1.1	9.1	11.395	0.194	405.7	6.9
	TF7	0.00002	0.00002	0.08493	0.00032	0.058	0.6	2.5	11.6	11.706	0.099	415.6	3.5
	TF8	0.00001	0.00001	0.08642	0.00024	0.037	0.2	3.0	14.6	11.543	0.068	410.4	2.4
	TF9	0.00005	0.00004	0.08477	0.00033	0.117	1.4	2.1	16.7	11.634	0.107	413.3	3.8
	TF10	0.00004	0.00001	0.08626	0.00084	0.072	1.2	83.2	100.0	11.458	0.045	407.7	1.6
JNC 663	TF1	0.00001	0.00000	0.08455	0.00332	0.007	0.4	4.8	4.8	11.779	0.192	417.9	6.8
Slate	TF2	0.00004	0.00000	0.08471	0.01031	0.027	1.3	4.3	9.1	11.650	0.211	413.8	7.5
	TF3	0.00004	0.00003	0.08440	0.00040	0.030	1.3	4.4	13.5	11.697	0.208	415.3	7.4
Average age:	TF4	0.00001	0.00002	0.08533	0.00025	0.066	0.4	4.8	18.3	11.675	0.189	414.6	6.7
416.2 ± 1.5 Ma	TF5	0.00002	0.00002	0.08531	0.00024	0.022	0.5	7.4	25.7	11.662	0.127	414.2	4.5
	TF6	0.00002	0.00001	0.08458	0.00072	0.023	0.5	7.8	33.5	11.766	0.121	417.5	4.3
	TF7	0.00001	0.00000	0.08454	0.00065	0.040	0.2	11.4	44.9	11.811	0.087	418.9	3.1
	TF8	0.00004	0.00003	0.08432	0.00049	0.029	1.3	14.3	59.2	11.703	0.059	415.5	2.1
	TF9	0.00003	0.00001	0.08464	0.00121	0.038	0.9	19.9	79.1	11.703	0.051	415.5	1.8
	TF10	0.00005	0.00002	0.08373	0.00067	0.036	1.6	21.0	100.0	11.751	0.048	417.0	1.7
JNC 542A	TF1	0.00025	0.00032	0.07861	0.00022	0.004	7.4	4.6	4.6	11.782	0.045	418.0	1.6
Phyllonite	TF2	0.00011	0.00005	0.08182	0.00072	0.007	3.3	7.0	11.6	11.814	0.042	419.0	1.5
	TF3	0.00014	0.00018	0.08091	0.00023	0.005	4.2	5.9	17.5	11.836	0.045	419.7	1.6
Average age:	TF4	0.00006	0.00002	0.08368	0.00097	0.003	1.8	9.2	26.7	11.732	0.039	416.4	1.4
417.1 ± 1.3 Ma	TF5	0.00008	0.00008	0.08297	0.00029	0.003	2.5	5.9	32.6	11.757	0.042	417.2	1.5
	TF6	0.00003	0.00000	0.08408	0.00201	0.004	0.8	4.3	36.9	11.795	0.045	418.4	1.6
	TF7	0.00005	0.00000	0.08313	0.00899	0.001	1.3	3.5	40.4	11.867	0.048	420.7	1.7
	TF8	0.00004	0.00001	0.08300	0.00170	0.000	1.3	5.2	45.6	11.893	0.045	421.5	1.6
	TF9	0.00007	0.00005	0.08171	0.00043	0.013	2.0	0.6	46.2	12.000	0.186	424.9	6.6
	TF10	0.00036	0.00003	0.07500	0.00224	0.000	10.6	4.2	50.4	11.918	0.048	422.3	1.7
	TF11	0.00002	0.00003	0.08365	0.00026	0.003	0.7	5.7	56.1	11.871	0.042	420.8	1.5
	TF12	0.00003	0.00003	0.08503	0.00026	0.021	0.8	44.1	100.0	11.672	0.039	414.5	1.4
JNC 649	1.4	0.00001	0.00001	0.08088	0.00031	0.272	0.2	6.9	6.9	12.341	0.068	435.6	2.4
Siltstone	1.6	0.00005	0.00006	0.08225	0.00027	0.253	1.4	18.7	25.6	11.985	0.031	424.4	1.1
	1.7	0.00002	0.00002	0.08225	0.00034	0.180	0.5	26.3	51.9	12.102	0.023	428.1	0.8
Total gas age:	2	0.00001	0.00000	0.08183	0.00152	0.274	0.2	8.6	60.5	12.200	0.057	**431.2**	**2.0**
435.7 ± 1.3 Ma	2.1	0.00027	0.00020	0.07401	0.00036	0.235	8.1	20.1	80.6	12.424	0.040	438.2	1.4
	2.2	0.00009	0.00009	0.08039	0.00029	0.275	2.5	8.6	89.2	12.127	0.059	**428.9**	**2.1**
	2.5	0.00008	0.00005	0.08037	0.00044	0.221	2.4	4.3	93.5	12.146	0.116	**429.5**	**4.1**
	2.6	0.00081	0.00000	0.06249	0.07581	0.218	23.8	2.2	95.7	12.188	0.272	**430.8**	**9.6**
	10	0.00050	0.00014	0.05290	0.00069	0.224	14.9	4.2	100.0	16.093	0.132	549.6	4.5
JNC 649	1.6	0.00005	0.00006	0.08124	0.00023	0.171	1.4	30.0	30.0	12.140	0.017	**429.3**	**0.6**
Siltstone	1.7	0.00004	0.00004	0.08120	0.00025	0.177	1.0	4.3	34.3	12.194	0.076	**431.0**	**2.7**
	1.9	0.00002	0.00001	0.08158	0.00096	0.157	0.5	16.3	50.6	12.200	0.025	**431.2**	**0.9**
Total gas age:	2.2	0.00003	0.00002	0.08104	0.00042	0.183	0.7	14.0	64.6	12.251	0.025	432.8	0.9
437.2 ± 1.2 Ma	2.6	0.00002	0.00003	0.08038	0.00025	0.235	0.6	21.8	86.4	12.363	0.020	436.3	0.7
	2.7	0.00005	0.00002	0.08044	0.00074	0.204	1.5	6.3	92.7	12.245	0.051	432.6	1.8
	3	0.00007	0.00003	0.07851	0.00067	0.154	1.9	3.3	96.0	12.491	0.091	440.3	3.2
	3.5	0.00016	0.00007	0.06756	0.00057	0.200	4.8	1.3	97.3	14.098	0.224	489.9	7.8
	8	0.00026	0.00030	0.05399	0.00017	0.192	7.6	2.7	100.0	17.117	0.115	579.5	3.9

Table 2. (*Cont.*)

Sample Rock or mineral	Step	$^{36}Ar/^{40}Ar$	$\pm 1\sigma$	$^{39}Ar/^{40}Ar$	$\pm 1\sigma$	Ca/K	^{40}Ar air (%)	^{39}Ar (%)		$^{40}Ar*/^{39}Ar_K$	$\pm 1\sigma$	Age (Ma)	$\pm 1\sigma$
Step-heating experiments													
JNC 663	1.3	0.00034	0.00007	0.12953	0.00230	0.052	9.9	3.4	3.4	6.953	0.140	258.2	5.2
Slate	1.5	0.00003	0.00001	0.08873	0.00137	0.036	0.7	9.9	13.3	11.185	0.042	399.0	1.5
	1.7	0.00008	0.00005	0.08307	0.00046	0.021	2.3	16.6	29.9	11.757	0.028	417.2	1.0
Total gas age:	1.9	0.00003	0.00004	0.08243	0.00028	0.033	1.0	43.0	72.9	12.010	0.014	**425.2**	**0.5**
418.0 ± 1.2 Ma	2.2	0.00006	0.00003	0.08216	0.00060	0.005	1.9	7.5	80.4	11.943	0.056	**423.1**	**2.0**
	2.5	0.00008	0.00002	0.08091	0.00154	0.007	2.4	5.1	85.5	12.064	0.079	**426.9**	**2.8**
	8	0.00005	0.00002	0.07900	0.00084	0.005	1.4	14.6	100.0	12.481	0.031	440.0	1.1
JNC 663	0.9	0.00042	0.00018	0.08396	0.00069	0.034	12.3	9.3	9.3	10.437	0.089	374.9	3.2
Slate	1	0.00000	0.00000	0.08747	0.00065	0.154	15.3	4.1	13.4	11.430	0.180	406.8	6.4
	1.1	0.00153	0.00019	0.04384	0.00129	0.137	45.3	0.9	14.3	12.481	0.868	440.0	30.6
Total gas age:	1.3	0.00001	0.00000	0.08577	0.00214	0.198	0.3	9.5	23.8	11.621	0.079	412.9	2.8
416.8 ± 1.4 Ma	1.7	0.00002	0.00001	0.08323	0.00080	0.178	0.7	17.7	41.5	11.934	0.045	**422.8**	**1.6**
	1.8	0.00004	0.00005	0.08310	0.00024	0.183	1.1	34.3	75.8	11.902	0.025	**421.8**	**0.9**
	2.2	0.00016	0.00004	0.07927	0.00111	0.174	4.8	7.3	83.1	12.010	0.107	**425.2**	**3.8**
	2.6	0.00000	0.00000	0.08442	0.00031	0.220	0.2	5.7	88.8	11.842	0.054	**419.9**	**1.9**
	3	0.00009	0.00001	0.07970	0.00195	0.289	2.5	10.9	99.7	12.239	0.071	432.4	2.5
	8	0.00002	0.00000	0.26048	0.00452	0.002	0.6	0.3	100.0	3.816	0.726	146.3	27.8
JNC 542A	1.3	0.00003	0.00002	0.08418	0.00045	0.005	0.8	42.2	42.2	11.785	0.011	418.1	0.4
Phyllonite	1.4	0.00007	0.00004	0.08421	0.00060	0.229	2.0	9.8	52.0	11.634	0.034	**413.3**	**1.2**
	1.5	0.00005	0.00004	0.08467	0.00040	0.379	1.3	29.5	81.5	11.656	0.020	**414.0**	**0.7**
Total gas age:	1.5	0.00003	0.00001	0.08537	0.00111	0.185	0.8	12.1	93.6	11.618	0.076	412.8	2.7
415.4 ± 1.2 Ma	1.6	0.00008	0.00002	0.08524	0.00124	0.469	2.2	2.4	96.0	11.480	0.118	**408.4**	**4.2**
	8	0.00012	0.00013	0.08256	0.00029	0.006	3.7	3.9	100.0	11.665	0.068	414.3	2.4
JNC 542A	1.3	0.00002	0.00002	0.08410	0.00030	0.005	0.7	19.5	19.5	11.807	0.014	**415.4**	**0.5**
Phyllonite	1.4	0.00003	0.00000	0.08253	0.00988	0.004	0.8	45.2	64.7	12.014	0.011	**421.9**	**0.4**
	1.4	0.00002	0.00000	0.08426	0.00131	0.006	0.6	32.7	97.4	11.794	0.011	**415.0**	**0.4**
Total gas age:	1.4	0.00052	0.00010	0.07376	0.00142	0.005	15.4	1.0	98.4	11.467	0.227	404.7	8.0
417.9 ± 0.3 Ma	2.1	0.00015	0.00007	0.08381	0.00068	0.003	4.5	1.1	99.5	11.391	0.207	402.3	7.3
	8	0.00018	0.00004	0.08488	0.00132	0.004	5.4	0.5	100.0	11.146	0.441	394.5	15.6

Ages in bold are those used for the calculation of a plateau age.

the entire time span chosen, between 400 and 460 Ma. This method thus avoids the risk of creating non-meaningful peaks, or missing important peaks out. The treatment relies on the hypothesis that the dated phases contain several sites with distinct isotopic composition, each of them therefore giving different, but geologically meaningful, age information. In the case of the Charnwood Forest samples analysed here, the largest reservoir (microscopically estimated at 70 to 92 %; Table 1) corresponds to micas that define the slaty cleavage microfabric, followed by replacive (3 to 20 %) and by detrital micas (5 to 10 %; Table 1). The expected ages of the deformation event would be given by the cleavage microfabric fine-grained white micas, as well as large proportions of the detrital and replacive micas, as discussed above. The fabric ages would correspond to the major peak in the cumulative probability diagrams (Fig. 3).

Ages determined by spot analyses range from 404.1 ± 1.9 to 452.7 ± 5.1 Ma, with two major clusters at *c.* 435 and *c.* 415 Ma (Table 2). For the Swithland Formation *in situ* samples (JNC 649, 659; Fig. 3a), the major peak is broad, with an age of 432.0 ± 7.2 Ma (10 spot analyses; MSWD = 1.01). For the Swithland Formation headstone samples, which are expected to be the most pure in terms of original mud content, one well-defined peak is present at 415.8 ± 4.0 Ma (n = 16; MSWD = 0.22), with a minor one on its left

flank (Fig. 3b). The Charnian ductile shear sample (JNC 542A) shows one single and well-defined peak at 419.4 ± 3.8 Ma (n = 10; MSWD = 1.60; Fig. 3c); this sample is significant because it is a tectonized igneous rock and so cannot have contained any detrital sedimentary components. All peaks defined in the probability density diagrams satisfy the goodness of fit criterion of MSWD lower than 2.5, as the calculated MSWD values range from 0.22 to 1.60.

Step-heating experiments were conducted on three samples from Charnwood Forest, each being analysed twice, and the results are presented in Figure 4. The spectra obtained are mostly flat, even though the first two to three steps of sample JNC 663 indicate significant superficial radiogenic argon loss; the higher ages of the last one or two steps in sample JNC 649 probably indicate the presence of inherited ^{40}Ar, and the first step of the duplicate analysis of sample JCN542A might suggest limited $^{39}Ar_K$ recoil (Fig. 4). These perturbations of the age spectra are to be expected with such fine-grained material as used here, where loss of both $^{40}Ar*$ and $^{39}Ar_K$ are to be expected. However, the obtained spectra permit the definition of plateau ages (based on at least three consecutive steps corresponding to more than 50 % of the gas) or the calculation of gas proportion-weighted average ages of relatively flat portions of the spectrum, ranging from 413.7 ± 1.2 Ma (sample JNC 542A, steps 2 to 5, 58 % of the gas) to
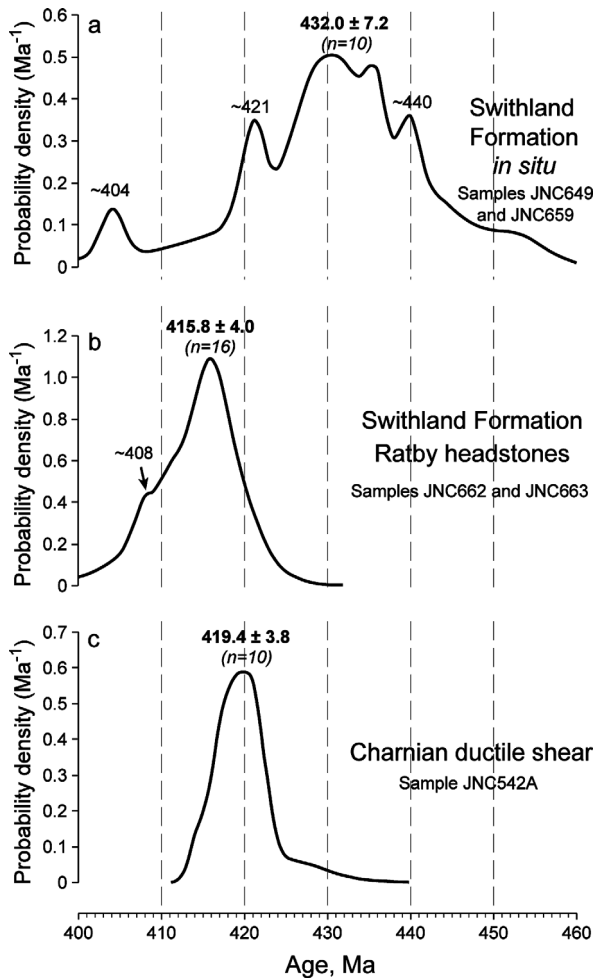
Figure 3. Cumulative probability diagrams for all ^{40}Ar–^{39}Ar spot analyses given in Table 2, organized by groups of dated samples, as indicated in the text. The age and error margin of each individual peak are indicated, together with the number of individual ages defining the relevant peak.
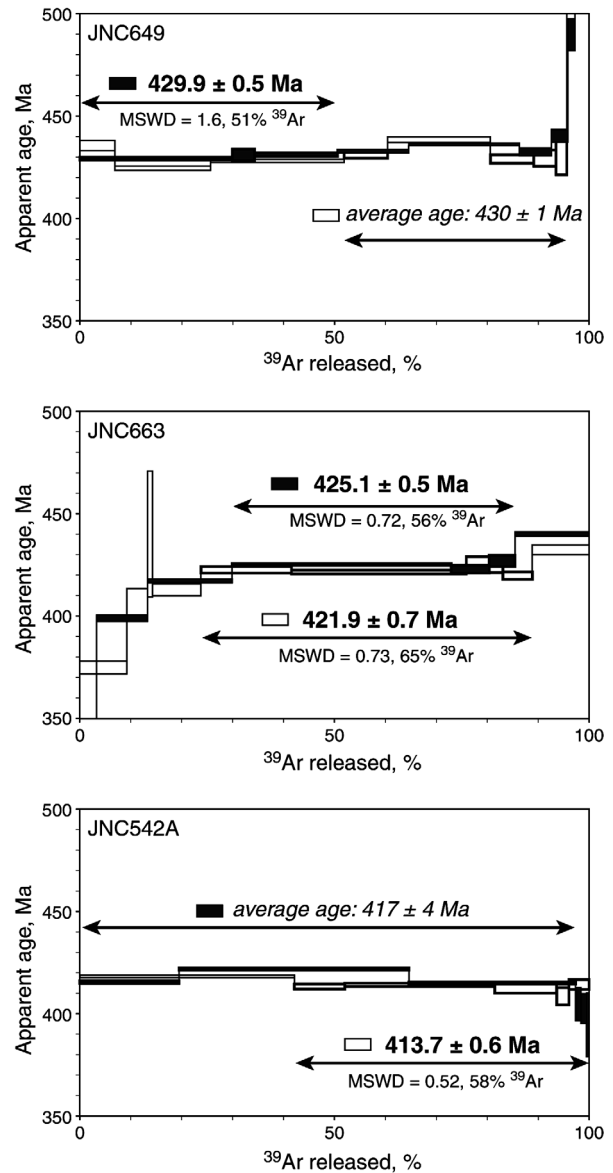

Figure 4. ^{40}Ar–^{39}Ar step heating age spectra of individual rock fragment slices. Note that the Charnwood samples yielded good age plateaus (see text for discussion).

429.9 ± 0.5 Ma (sample JNC 649, steps 1 to 3, 51 % of the gas). The ages obtained by double analyses are consistent, even though they do not overlap at the 1σ uncertainty level (Fig. 4).

In summary, the step-heating results closely reflect the spot analyses in revealing two age groupings: the main one at *c.* 425 to 416 Ma (three plateau ages and an average age from samples JNC 542A and JNC 663) and a further one at *c.* 430 Ma (sample JNC 649). It is important to note that for sample JNC 649 the step-heating analysis (Fig. 4) and the majority of single spot analyses (Fig. 3a) give very similar ages of *c.* 430 Ma and 432 Ma, respectively.

7. Discussion and interpretation of the age data

The spread of the ^{40}Ar–^{39}Ar age data gives a Silurian to earliest Devonian age range, between 432 and 416 Ma, for Charnwood samples. Of the two age groupings represented within this cluster, the younger one, of *c.* 425 to 416 Ma, which is both well defined (Fig. 3) and present in all dated samples (see also

Table 2), is interpreted to constrain the age of the main deformational event, which included metamorphism, folding, ductile shearing and the development of the penetrative cleavage. This age grouping was obtained from single-spot and step-heating analyses, and it indicates a Silurian (Wenlock) to earliest Devonian (Lochkovian) age on the timescale of Gradstein *et al.* (2005). It is important to stress that the three purest samples, in terms of tectonic mica content, are represented within this younger age grouping; they were collected from Swithland Formation headstones (two samples; JNC 662, 663) and a ductile shear zone cutting igneous rocks (one sample; JNC 542A) and they give well-defined age peaks at 415.8 ± 4.0 and 419.4 ± 3.8 Ma, respectively (Fig. 3b, c).

The deformational event at *c.* 425–416 Ma that is constrained by the new ^{40}Ar–^{39}Ar determinations does not contradict the possibility of an Early Cambrian

age recently proposed for the Swithland Formation (Bland & Goldring, 1995; McIlroy, Brasier & Moseley, 1998). The new age estimate does, however, rule out a recent proposal by Compston, Wright & Toghill (2002) that the cleavage deformation could have arisen during earliest Cambrian time. A metamorphic hiatus, implying weak deformation, probably did originally exist between the Neoproterozoic Charnian Supergroup and ?Early Cambrian strata of the Swithland Formation, by analogy with the situation in the Midland Microcraton's interior exposed at Nuneaton (Fig. 1a). There, deep diagenetic zone sedimentary rocks of Early Cambrian age unconformably overlie relatively higher grade (lower anchizonal) rocks of the Caldecote Volcanic Formation, equated with the Charnian Supergroup (Bridge *et al.* 1998; Merriman *et al.* 1993). In Charnwood Forest, however, the evidence for this metamorphic discontinuity would have been obliterated by the subsequent epizonal recrystallization of the Neoproterozoic and Early Cambrian rocks documented here.

The older (Silurian) age grouping at *c.* 432–430 Ma for the *in situ* Swithland Formation may reflect the imprint of an earlier thermal event. The much lower age values, of *c.* 404 Ma and *c.* 408 Ma, most probably correspond to the effects of argon loss due to perturbations in the isotopic system, as they are defined by a very limited number of analyses.

8. Regional implications

Given the limitations of the whole-rock dating methods employed, these data have provided a Silurian to Early Devonian estimate for the age of Charnwood deformation, which is significantly older than Acadian deformational ages recorded elsewhere in southern mainland Britain. For example, within the paratectonic Caledonides belts to the west and north of the Midlands Microcraton (Fig. 1a), Sherlock *et al.* (2003) used ^{40}Ar–^{39}Ar laser microprobe analysis to date pressure fringe white mica, giving a mean age of 396.1 $\pm$ 1.4 Ma for the Acadian cleavage. Farther north, a similar cleavage age of 397 $\pm$ 7 Ma was obtained from a Silurian mid-anchizonal grade metabentonite in the Ribblesdale inlier (Fig. 1a) of northern England (Merriman *et al.* 1995*b*). There, however, an Rb–Sr isochron age of 465 $\pm$ 10 Ma has also been determined, suggesting the possibility that earlier, diagenetic or metamorphic events may survive penetrative cleavage deformation (Dodson & Robinson, 2006). The *c.* 397 Ma age determinations constrain the peak of Acadian metamorphism and deformation to latest Emsian time, according to the U–Pb chronology for this part of the Devonian suggested by Kaufmann *et al.* (2005).

Although more work clearly needs to be carried out on the Charnwood rocks, our preliminary findings suggest that their argon reservoirs could have been influenced by the events that accompanied closure of the Iapetus Ocean, towards the end of the Silurian
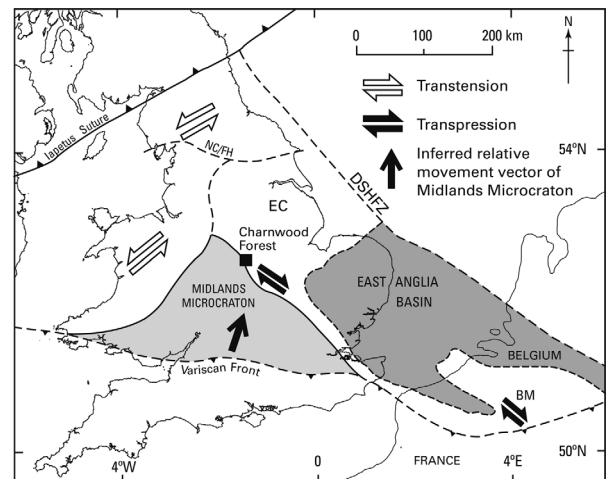
Figure 5. Proposed tectonic setting during the *c.* 425–416 Ma deformation in Charnwood Forest. Major basement terranes are: EC – Eastern Caledonides; BM – Brabant Massif. Structural lineaments are: NC/FH – North Craven/Flamborough Head fault system; DSHFZ – Dowsing–South Hewett Fault Zone. Other information is given in Figure 1a. Data sources are from compilations by Pharaoh (1999), Soper & Woodcock (2003) and Van Grootel *et al.* (1997).

Period. According to Soper & Woodcock (2003), a 'sizeable time gap' is present between Iapetus closure and the onset of Acadian deformation. Within this pre-Acadian tectonic regime (Fig. 5), a changeover from sinistral convergence to sinistral transtension occurred at about 420 Ma in the Welsh Basin and Lake District regions of southern Britain (Soper & Woodcock, 2003), roughly coinciding with the younger estimated age range for the Charnwood deformation. Further afield, the Charnwood event may also have parallels in a *c.* 425–414 Ma 'Neo-Acadian' tectonic imprint recognized in the Avalonian terranes of the USA (Robinson *et al.* 1998). The main Acadian deformational event in southern Britain has been attributed to transpression caused by the subsequent collision of Armorica with the terranes of Laurentia, Avalonia (the Early Palaeozoic microcontinent) and Baltica that had previously been docked along the Iapetus closure line (Soper, Webb & Woodcock, 1987; Dewey & Strachan, 2003).

An attempt has been made to clarify the mechanism that caused the Charnwood deformation, in order to compare it with Acadian structural styles in the Welsh Basin and northern England. The Charnwood cleavage orientation is slightly sinuous, bearing ESE (100° to 120°) and cutting obliquely across the SE axial trend of the main Charnwood anticline (Fig. 1b). This was described by J. Moseley (unpub. Ph.D. thesis, Univ. Leicester, 1979) as an anticlockwise cleavage transection, and in order to constrain it further, detailed measurements of fold/cleavage relationships in the Charnian Supergroup were made by TCP and JNC. It was found that the fold-girdle representing the best fit to bedding poles is offset from the mean cleavage pole (and the regional fold-axis predicted from the fold-girdle

likewise offset from the observed bedding on cleavage intersections) by an angle of 8°, confirming anticlockwise transection (Fig. 1c). These relationships suggest that the Charnwood deformation arose within a prevailing regime of dextral transpression. It is noteworthy that in the paratectonic Caledonides domains to the west and north of the Midlands Microcraton, the Acadian event produced a transecting cleavage generated within a sinistral transpressional regime. These younger, Acadian structures were attributed to the northwards movement of the Midlands Microcraton as a rigid indenter (Soper, Webb & Woodcock, 1987; Woodcock, 1990).

To account for these different ages and styles of transection geometry on either side of the Midlands Microcraton, it is suggested that the ^{40}Ar–^{39}Ar age estimate of 425–416 Ma in Charnwood Forest may include the record of early deformation in the assemblage of terranes that, south of the Scottish Highlands, were converging with the Iapetus Ocean suture line (Fig. 1a). It is possible that, as sinistrally oblique accretion in the Scottish Southern Uplands was slowing down (Soper & Woodcock, 2003), dextral transpressive deformation in Charnwood Forest was commencing along the NE margin of the Midlands Microcraton indenter, perhaps documenting the latter's early relative northward movement against the Eastern Caledonides terrane. This involvement of the microcraton is broadly compatible with the concept (Soper & Woodcock, 2003) of sinistral transtension prevailing across Wales and NW England at that time (Fig. 5). Uplift of the microcraton eastern margin, perhaps commensurate with the Charnwood deformation, would also be in keeping with an upwards shallowing of depositional facies, reddening of strata and possible cessation of deposition of sediments within the East Anglia Basin, in which the youngest biostratigraphically dated strata are of Silurian, late Přídolí age (Woodcock & Pharaoh, 1993), or about 416 Ma on the timescale of Gradstein *et al.* (2005). This transition from marine to non-marine deposition is also seen across the whole of the western edge of the microcraton, into the Welsh Basin and as far north as the Lake District, as reviewed in Soper & Woodcock (2003); it is the evidence formerly used to suggest that the 'Caledonian Orogeny' was end-Silurian in age.

It is noteworthy that in the paratectonic Eastern Caledonides domain immediately to the east of Charnwood Forest (Fig. 1a), Cambro-Ordovician basement rocks intersected in boreholes differ from the Charnwood rocks in possessing generally weaker tectonic fabrics and lower, anchizonal KI values, corresponding to a maximum burial of approximately 8 km depth (Kemp, 1997; Pharaoh *et al.* 1987; Merriman *et al.* 1993; Van Grootel *et al.* 1997). Thus the style of Charnwood deformation, and its epizonal metamorphism, could represent a narrow zone of relatively deeper burial and stronger compression that was localized along the tectonic boundary between the Eastern Caledonides and Midlands Microcraton.

Within the continuation of the Eastern Caledonides belt in Belgium, dextral transpressive deformation has been tentatively suggested (Sintubin, Brodkom & Laduron, 1998), and the Charnwood deformation reported here thus fulfils their prediction that such a tectonic regime should be widespread within the 'Anglo-Brabant fold-belt', which encompasses the Eastern Caledonides and Brabant Massif terranes (Fig. 5). The Brabant deformation appears to have been particularly protracted, compared with the areas of southern Britain affected by the Acadian event (Debacker *et al.* 2005; Woodcock, Soper & Strachan, 2007). On the basis of unconformities, a relatively young 'Acadian' Brabantian event has been suggested, between earliest Devonian (Late Lochkovian) and Givetian times (Van Grootel *et al.* 1997). However, radiometric age determinations (^{40}Ar–^{39}Ar) on cleavage-parallel micas (Dewaele, Boven & Muchez, 2002; Debacker *et al.* 2005) indicate an earlier phase of Brabantian deformation, with one age cluster at 419–412 Ma (Přídolí and Lochkovian), overlapping with that seen in Charnwood Forest, and another at 407–401 Ma (Emsian).

9. Conclusions

In Charnwood Forest, spot analysis and step-heating experiments suggest the presence of two distinct ^{40}Ar–^{39}Ar argon age clusters: an older and diffuse one peaking at around 432–430 Ma (Llandovery) and a younger grouping at 425 to 416 Ma (Wenlock–Lochkovian). The younger grouping is represented in all datasets and is regarded as the best estimate for the age of the deformation. In three of the samples it is characterized by well-defined peaks, at 419 and 416 Ma (Přídolí–Lochkovian), the former value having been determined for a cleavage-related ductile shear zone cutting primary igneous lithologies. The cleavage arose within a dextral transpressional regime and was a consequence of burial and compression localized within or adjacent to the tectonic interface between the Eastern Caledonides structural province and the NE margin of the Midlands Microcraton. A similar age of cleavage deformation has been detected in the Brabant continuation to the Eastern Caledonides belt in Belgium, and this 'Brabantian' phase of the Caledonian Orogeny evidently overlaps with a period of transtension in western Britain. Although further work will be required in order to bracket more precisely the timing of Charnwood deformation, the Silurian to earliest Devonian age estimate suggests that folding, cleavage and epizonal metamorphism could be related to Iapetus closure, perhaps overlapping with the final stages of that event. The eastern margin of the Midlands Microcraton indenter could therefore have been tectonically active some 20–30 Ma before the widespread Acadian Phase (Devonian: Emsian) of the Caledonian orogeny that occurred further west, in the Welsh Basin and Lake District.

References

ALEXANDRE, P., CHALOT-PRAT, F., SAINTOT, A., WIJBRANS, J., STEPHENSON, R., WILSON, M., KITCHKA, A. & STOVBA, S. 2004. ^{40}Ar/^{39}Ar dating of magmatic activities in the Donbas Foldbelt and the Scythial Platform (Eastern European Craton). *Tectonics* **23**(5), TC5002, 15 pp.

BLAND, B. H. & GOLDRING, R. 1995. *Teichichnus rectus* Seilacher from the Charnian of Leicestershire. *Neues Jahrbuch für Geologie und Paläontologie Abhandlungen* **195**, 5–23.

BRIDGE, D. MCC., CARNEY, J. N., LAWLEY, R. S. & RUSHTON, A. W. A. 1998. *The geology of the country around Coventry and Nuneaton.* Memoir of the British Geological Survey Sheet 169 (England and Wales), 185 pp.

BRITISH GEOLOGICAL SURVEY. 1996. *Tectonic map of Britain, Ireland and adjacent areas, 1:500 000* (compilers T. C. Pharaoh, J. H. Morris, C. B. Long & P. D. Ryan). Keyworth, Nottingham: British Geological Survey.

CARNEY, J. N. 1999. Revisiting the Charnian Supergroup: new advances in understanding old rocks. *Geology Today* **15**(6), 221–9.

CARNEY, J. N. 2005. Old Cliffe Hill and Whitwick quarries, Charnwood Forest. *Mercian Geologist* **16**, 138–41.

COMPSTON, W., WRIGHT, A. E. & TOGHILL, P. 2002. Dating the Late Precambrian volcanicity of England and Wales. *Journal of the Geological Society, London* **159**, 323–39.

DALRYMPLE, G. B., ALEXANDER, E. C. JR, LANPHERE, M. A. & KRAKER, G. P. 1981. Irradiation of samples for ^{40}Ar/^{39}Ar dating using the Geological Survey TRIGA reactor. *U.S. Geological Survey Professional Paper*, Report P1176, 55 pp.

DEBACKER, T. N., DEWAELE, S., SINTUBIN, M., VERNIERS, J., MUCHEZ, P. & BOVEN, A. 2005. Timing and duration of the progressive deformation of the Brabant Massif, Belgium. *Geologica Belgica* **8**, 20–34.

DEWAELE, S., BOVEN, A. & MUCHEZ, P. H. 2002. ^{40}Ar/^{39}Ar dating of mesothermal, orogenic mineralization in a low-angle reverse shear zone in the Lower Palaeozoic of the Anglo-Brabant fold belt, Belgium. *Transactions of the Institution of Mining and Metallurgy* **111**, B215–20.

DEWEY, J. F. & STRACHAN, R. A. 2003. Changing Silurian–Devonian relative plate motion in the Caledonides: sinistral transpression to sinistral transtension. *Journal of the Geological Society, London* **160**, 219–29.

DODSON, M. H. & ROBINSON, D. 2006. A mid-Ordovician Rb–Sr isochron age from the Ingleton Group, North Yorkshire: metamorphism or diagenesis? *Proceedings of the Yorkshire Geological Society* **56**(2), 81–5.

DONG, H., HALL, C. M., HALLIDAY, A. N., PEACOR, D. R., MERRIMAN, R. J. & ROBERTS, B. 1997. ^{40}Ar/^{39}Ar dating of Late Caledonian (Acadian) metamorphism and cooling of K-bentonites and slates from the Welsh Basin, U.K. *Earth and Planetary Science Letters* **150**, 337–51.

GRADSTEIN, F. M., OGG, J. G., SMITH, A. G. *et al.* 2005. *A Geologic Time Scale, 2004.* Cambridge University Press, 589 pp.

HO, N.-C., PEACOR, D. R. & VAN DER PLUIJM, B. A. 1999. Preferred orientation of phyllosilicates in Gulf Coast mudstones and relation to the smectite–illite transition. *Clays and Clay Minerals* **47**, 495–504.

KAUFMANN, B., TRAPP, E., MEZGER, K. & WEDDIGE, K. 2005. Two new Emsian (Early Devonian) U–Pb zircon ages from volcanic rocks of the Rhenish Massif (Germany): implications for the Devonian time scale. *Journal of the Geological Society, London* **162**, 363–71.

KEMP, S. J. 1997. The nature and maturity of mudstone intervals from the Ticknall borehole, Derbyshire. *British Geological Survey Technical Report* **WG/97/18**, 18 pp.

KEMP, S. J. & MERRIMAN, R. J. 1995. White mica (illite) crystallinity of Charnian rocks from the Loughborough district (1:50000 geological sheet 141). *British Geological Survey Technical Report* **WG/95/7**, 12 pp.

KISCH, H. J. 1990. Calibration of the anchizone: a critical comparison of illite 'crystallinity' scales used for definition. *Journal of Metamorphic Geology* **8**, 31–46.

KNIPE, R. J. 1981. The interaction of deformation and metamorphism in slates. *Tectonophysics* **78**, 249–72.

LEE, M. K., PHARAOH, T. C. & SOPER, N. J. 1990. Structural trends in central Britain from images of gravity and aeromagnetic fields. *Journal of the Geological Society, London* **147**, 241–58.

LI, G., PEACOR, D. R., MERRIMAN, R. J. & ROBERTS, B. 1994. The diagenetic to low-grade metamorphic evolution of matrix white micas in the system muscovite–paragonite in a mudrock from Central Wales, U.K. *Clays and Clay Minerals* **42**, 369–81.

MCDOUGALL, I. & ROKSANDIC, Z. 1974. Total fusion ^{40}Ar/^{39}Ar ages using the HIFAR reactor. *Journal of the Geological Society of Australia* **21**, 81–9.

MCILROY, D., BRASIER, M. D. & MOSELEY, J. M. 1998. The Proterozoic–Cambrian transition within the 'Charnian Supergroup' of central England and the antiquity of the Ediacaran fauna. *Journal of the Geological Society, London* **155**, 401–12.

MCKERROW, W. S., MAC NIOCAILL, C. & DEWEY, J. F. 2000. The Caledonian Orogeny redefined. *Journal of the Geological Society, London* **157**, 1149–55.

MENEISY, M. Y. & MILLER, J. A. 1963. A geochronological study of the crystalline rocks of Charnwood Forest, England. *Geological Magazine* **100**, 507–23.

MERRIMAN, R. J. & KEMP, S. J. 1997. Metamorphism of the Charnian Supergroup in the Loughborough district, 1:50000 Sheet 141. *British Geological Survey Technical Report* **WG/97/7**, 12 pp.

MERRIMAN, R. J. & PEACOR, D. R. 1999. Very low-grade metapelites: mineralogy, microfabrics and measuring reaction progress. In *Low-Grade Metamorphism* (eds M. Frey & D. Robinson), pp. 1–60. Blackwell Science.

MERRIMAN, R. J., PHARAOH, T. C., WOODCOCK, N. H. & DALY, P. 1993. The metamorphic history of the concealed Caledonides of eastern England and their foreland. *Geological Magazine* **130**, 613–20.

MERRIMAN, R. J., REX, D. C., SOPER, N. J. & PEACOR, D. R. 1995*b*. The age of Acadian cleavage in northern England, UK: K–Ar and TEM analysis of a Silurian metabentonite. *Proceedings of the Yorkshire Geological Society* **50**, 255–65.

MERRIMAN, R. J., ROBERTS, B. & PEACOR, D. R. 1990. A transmission electron microscope study of white mica crystallite size distribution in a mudstone to slate

transitional sequence, North Wales, U.K. *Contributions to Mineralogy and Petrology* **106**, 27–40.

MERRIMAN, R. J., ROBERTS, B., PEACOR, D. R. & HIRONS, S. R. 1995*a*. Strain-related differences in the crystal growth of white mica and chlorite: a TEM and XRD study of the development of metapelitic microfabrics in the Southern Uplands thrust terrane, Scotland. *Journal of Metamorphic Geology* **13**, 559–76.

MOSELEY, J. & FORD, T. D. 1985. A stratigraphic revision of the Late Precambrian rocks of the Charnwood Forest, Leicestershire. *Mercian Geologist* **10**, 1–18.

PARRY, W. T., BUNDS, M. P., BRUHN, R. L., HALL, C. M. & MURPHY, J. M. 2001. Mineralogy, ^{40}Ar/^{39}Ar dating and apatite fission track dating of rocks along the Castle Mountain faults, Alaska. *Tectonophysics* **337**, 149–72.

PHARAOH, T. C. 1999. Palaeozoic terranes and their lithospheric boundaries within the Trans-European Suture Zone (TESZ): a review. *Tectonophysics* **314**, 17–41.

PHARAOH, T. C., MERRIMAN, R. J., WEBB, P. C. & BECKINSALE, R. D. 1987. The concealed Caledonides of eastern England: preliminary results of a multidisciplinary study. *Proceedings of the Yorkshire Geological Society* **46**, 355–69.

PHARAOH, T. C. & CARNEY, J. N. 2000. Introduction to the Precambrian rocks of England and Wales. In *Precambrian Rocks of England and Wales* (eds J. N. Carney, J. M. Horák, T. C. Pharaoh *et al.*), pp. 3–17. Geological Conservation Review Series no. 20. Peterborough: Joint Nature Conservation Review Committee.

RENNE, P. R., SWISHER, C. C., DEINO, A. L., KARNER, D. B., OWENS, T. L. & DEPAOLO, D. J. 1998. Intercalibration of standards, absolute ages and uncertainties in ^{40}Ar/^{39}Ar dating. *Chemical Geology* **145**, 117–52.

ROBINSON, P., TUCKER, R. D., BRADLEY, D., BERRY, H. N. & OSBERG, P. H. 1998. Palaeozoic orogens in New England, USA. *GFF* **20**, 119–48.

SHERLOCK, S. C., KELLEY, S. P., ZALASIEWICZ, J., SCHOFIELD, D., EVANS, J., MERRIMAN, R. J. & KEMP, S. J. 2003. Precise dating of low-temperature deformation: Strain-fringe analysis by ^{40}Ar–^{39}Ar laser microprobe. *Geology* **31**, 219–22.

SINTUBIN, M., BRODKOM, F. & LADURON, D. 1998. Cleavage-fold relationships in the Lower Cambrian Tubize Group, southeast Anglo-Brabant Fold Belt (Lembeek, Belgium). *Geological Magazine* **135**, 217–26.

SMITH, N. J. P. 1987. The deep geology of central England: the prospectivity of the Palaeozoic rocks. In *Petroleum Geology of North West Europe* (eds J. Brooks & K. Glennie), pp. 217–24. London: Graham & Trotman.

SOPER, N. J., WEBB, B. C. & WOODCOCK, N. H. 1987. Late Caledonian (Acadian) transpression in north-west England: timing, geometry and geotectonic significance. *Proceedings of the Yorkshire Geological Society* **46**, 175–92.

SOPER, N. J. & WOODCOCK, N. H. 2003. The lost Old Red Sandstone of England and Wales: a record of post-Iapetan flexure of Early Devonian transtension? *Geological Magazine* **140**, 627–47.

TURNER, J. S. 1949. The deeper structure of central and northern England. *Proceedings of the Yorkshire Geological Society* **27**, 280–97.

VAN DE PLUIJM, B. A., HO, N.-C., PEACOR, D. R. & MERRIMAN, R. J. 1998. Contradictions of slate formation resolved. *Nature* **392**, 348.

VAN GROOTEL, G., VERNIERS, J., GEERKENS, B., LADURON, D., VERHAEREN, M., HERTOGEN, J. & DE VOSS, W. 1997. Timing of magmatism, foreland basin development, metamorphism and inversion in the Anglo-Brabant fold belt. *Geological Magazine* **134**, 607–16.

VILLA, I. M. 1998. Isotopic closure. *Terra Nova* **10**, 42–7.

WARR, L. N. & RICE, A. H. N. 1994. Interlaboratory standardization and calibration of clay mineral crystallinity and crystallite size data. *Journal of Metamorphic Geology* **12**, 141–52.

WINCHESTER, J. A., PHARAOH, T. C. & VERNIERS, J. 2002. Palaeozoic amalgamation of Central Europe: an introduction and synthesis of new results from recent geological and geophysical investigations. In *Palaeozoic amalgamation of Central Europe* (eds J. A. Winchester, T. C. Pharaoh & J. Verniers), pp. 1–18. Geological Society of London, Special Publication no. 201.

WOODCOCK, N. H. 1990. Transpressive Acadian deformation across the Central Wales Lineament. *Journal of Structural Geology* **12**, 329–37.

WOODCOCK, N. H. & PHARAOH, T. C. 1993. Silurian facies beneath East Anglia. *Geological Magazine* **130**, 681–90.

WOODCOCK, N. H., SOPER, N. J. & STRACHAN, R. A. 2007. A Rheic cause for Acadian deformation in Europe. *Journal of the Geological Society, London* **164**, 1023–36.